Original Articles

Hydrodynamic parameters of floods and related bank erosion events indicated from tree rings and 2D hydrodynamic model for a small ungauged catchment (Sudeten Mts., Poland)

Ireneusz Malik [a,*], Małgorzata Wistuba [a], Damian Absalon [a], Michał Habel [b], Sergey Chalov [c], Ruide Yu [a,d]

[a] University of Silesia in Katowice, Institute of Earth Sciences, Polish-Chinese Centre for Environmental Research, 60 Będzińska, 41-200 Sosnowiec, Poland
[b] Kazimierz Wielki University, Institute of Geography, 30 Chodkiewicza, 85-064 Bydgoszcz, Poland
[c] Lomonosov Moscow State University, Faculty of Geography, 1 Leninskiye Gory, 119991 Moscow, Russia
[d] Chinese Academy of Sciences, Xinjiang Institute of Ecology and Geography, No.818 South Beijing Road, Urumqi, Xinjiang 830011, China

ABSTRACT

Small mountain catchments usually lack hydrological monitoring and gauges. Therefore, in such areas, data on past flood and bank erosion are often missing, which makes assessing flood and erosion hazards very limited. We attempt to fill in this gap by dating individual flood and erosion events from growth disturbances produced by trees after their stems are tilted, and their roots are exposed and wounded by transported material. We aimed to develop a conceptual approach to integrate dendrochronology and 2D modelling for indicating and assessing past events of floods and bank erosion on a small mountain river Łomniczka, Sudeten mountains, Poland. We dated growth disturbances resulting from tilting of stems of spruce trees which grow on eroded riverbanks, i.e. tree-ring eccentricity and compression wood. We also dated disturbances resulting from the exposure of roots from under the soil cover, i.e. sudden decreases of cell lumen, and root injuries by debris transported by floods, i.e. scars and traumatic resin ducts. Dendrochronology allow to indicate the occurrence of 28 floods since the 1930s, including 11 floods when bank erosion was also recorded at study sites. The approach enables to identify rates of bank erosion during specific floods which ranged at study sites from 20 to 120 cm. The largest discharge was determined for the 1997 flood ($106,7 \ m^3 \ s^{-1}$), and the highest flow velocities were obtained for the 1930 floods (4.59 m/s). Results show that the highest shear stress occurred during the floods in 1943 and 1977 ($510,3 N/m^2$) and in 1997 flood ($469.1 \ N/m^2$). We conclude that dendrochronology combined with 2D modelling allowed us to indicate past floods and bank erosion, and to prepare reliable inventories for analyses of flood and erosion hazard. The approach proposed in this paper can also be used as a tool for flood management, spatial management and planning.

1. Introduction

Indication of floods and events of bank erosion in ungauged catchments is often limited by the lack of hydrological data. Hydrological monitoring is usually missing in small mountain catchments. Therefore, such areas are often omitted in studies on floods and erosion. Flood indication and flood-hazard assessments are most often based on gauges and post-flood surveys from larger river valleys (Büchele et al., 2006; Marchi et al., 2010; Salehi-Hafshejani et al., 2019; Ostad-Ali-Askari and Shayannejad, 2021). Extrapolating data from large valleys to smaller,

distant upstream catchments can be a source of errors, mainly due to significant spatial variability of rainfall and flood conditions. Difficulties in modelling floods in small river catchments and valleys often make results of modelling inaccurate and increase risk of flood damages in valley floors (Norbiato et al., 2008; Merz et al., 2010; Mazzorana et al., 2013; Ostad-Ali-Askari et al., 2017; Pirnazar et al., 2018). At the same time, examples of damages caused by flooding in small catchments are frequent (e.g. Llasat et al., 2003; Vinet, 2008). During floods, bank erosion often occurs and poses an additional threat to buildings and infrastructure (Lawler, 1993). During particularly large floods, bank

erosion can undermine and destroy buildings and roads (Baishya, 2013).

The rate of bank erosion can be estimated from changes in the position of the river channel (Mili et al., 2013), e.g. by comparing maps of diverse age (in particular maps made before and after a flood, by repeated GPS survey (Wu and Cheng, 2005) or orthogonal reference system fixed by erosion pins (Vandekerckhove et al., 2001a). However, these methods allow to indicate only relatively recent events of erosion. Past events of bank erosion and, thus, past floods can be studied with dendrochronology, provided that trees grow in the valley bottom (Stoffel et al., 2012).

In the temperate climatic zone, small mountain catchments are usually forested, which makes it possible to yield information on past floods from annual tree rings. Dendrochronological data can also be applied to study flood hazard (Ballesteros-Cánovas et al., 2015). Botanical evidences of floods were initially described by Sigafoos (1964) who dated stem injures and sprouts growing from tilted and wounded trees. He also established a tree-ring reconstruction of flood frequency. Also, Harrison and Reid (1967) dated scars on trees to study flood frequency and magnitude, while Helley and LaMarche (1968) used dendrochronology to indicate floods during the past 400 years.

Dendrochronology has been proved to provide high precision of indication of floods and erosion. In particular, this concerns indication of floods based on wood anatomy, e.g. on changes in the size of wood vessels (e.g. Yanosky, 1984; Arbellay et al., 2012; Wertz et al., 2013) and the changes of wood anatomy after a root is exposed from under the soil cover (Gärtner et al., 2001; Hitz et al., 2008; Corona et al., 2011; Stoffel et al., 2013). There are many examples of studies on floods in small, ungauged catchments, which benefitted from the precision of tree-ring indication. E.g. Zielonka et al. (2008) dated scars on riparian trees which were injured during floods in the Tatra Mts., Poland. Ruiz-Villanueva et al. (2010) used several types of growth disturbances to date flash floods on Pelayo River, Central Spain and Šilhán (2015) dated flash floods in small ungauged catchments in the Carpathian Mts, Czech Republic. There are also many examples of erosion events dated from tree rings (LaMarche, 1966; Carrara and Carroll, 1979; Bodoque et al., 2005; Pelfini and Santilli, 2006; Fantucci, 2007; Malik and Matyja, 2008; Bollati et al., 2012).

Besides the simple indication of floods, dendrochronology can also be applied to reconstruct the magnitude and frequency of floods and groundwater levels and river discharges (Gholami et al., 2015; Zhou et al., 2019; Hunter et al., 2020). Ballesteros Cánovas et al. (2011); Ballesteros-Cánovas et al. (2015) reconstructed flood peak discharges from measurements of scar elevation on tree stems and two 2D hydraulic modeling. With a high number of dendrochronological datings obtained from one area, it is even possible to indicate changes of riverbed or gully topography (Malik, 2006; Malik, 2008). It is also possible to estimate the role of individual floods in bank erosion by determining the rate of erosion during individual events (Malik and Matyja, 2008). However, dendrochronological analyses of erosion have also some limitations, e.g. recent events of erosion can destroy the record of older events and prevent precise indication of their impact on riverbed relief (Stoffel et al., 2013).

As a reliable tool for indicate past events of erosion, dendrochronology is no enough to assess hydrodynamic parameters of individual floods. This issue can be solved if additional tools of hydrodynamic modelling are applied. At the same time, according to our knowledge, dendrochronology and 2D (Two-Dimensional) modelling have never before been combined to estimate hydraulic parameters of bank erosion. Hydrodynamic parameters can also be estimated with hydraulic models. These models allow to conclude on both flooding and erosion in individual sections of the river channel, i.e. to estimate discharges, velocities of water flow and shear stresses. Various hydraulic models are developed to enable simulation and forecasting hydrodynamic parameters (Hassan et al., 2005; Kleinhans, 2005; Wu et al., 2005; Bhuiyan et al., 2015; Morianou et al., 2018; Ostad-Ali-Askari et al., 2020; Derakhshannia et al., 2020). Two- and three-dimensional models have the

advantage of simulating flow propagation and morphological parameters with high accuracy (Ghanem et al., 1996; Shen and Diplas, 2008). The most widely used 2D modelling software packages are MIKE 21C (DHI and MIKE 21C, 2011), FLOW 2D (O'Brien, 2006) and CCHE2D hydrodynamic model (Tongbi et al., 2017). The two-dimensional Mike 21C model is a suitable tool for quick and detailed simulation of changes in river hydraulics and river morphology (Morianou et al., 2018; Ostad-Ali-Askari et al., 2019; Golian et al., 2020).

The main novelty of the study is using simultaneously chosen wood anatomy features and 2D modelling for calculation not only hydrological parameters (discharge, flow velocity) but also erosion parameters (shear stress). To the best of our knowledge, such studies have not been conducted before. Using dendrochronology and 2D modelling simultaneously allows to more precisely reconstruction floods and bank erosion events. In case of ungauged streams, there is no other possibility of reliable reconstruction of hydrogeomorphic parameters.

This study aims to indicate erosion events and estimate hydrodynamic parameters of related individual floods based on tree ring data. Therefore, the study focuses at dating individual floods and related bank erosion events from tree rings as a basis for further 2D modelling. We aimed to estimate rates of bank erosion and water levels during individual events of erosion dated from tree rings in selected valley cross-sections (1); we also aimed to calculate selected hydrodynamic parameters (discharge, flow velocity, shear stress) for individual events of erosion with 2D modelling (2). We chose these parameters because they are available for automatic calculation in Mike 21 software. In addition, they are adapted to other steps which are configured in the software. We selected the MIKE 21C model for this study because it can be used in a montane river setting, with valley floor characterized by high roughness causing local changes in the velocity and direction of water flow (Morianou et al., 2018). We used a 2D model because using a 3D model for the proposed research would be disadvantageous. The 3D model is used in sections of rapidly changing water flows, e.g. around bridge pillars, embankments, weirs (Wu et al., 2004). For riverbed erosion analyzes, it would be necessary to convert 3D models (internal module) into 2D views (external module). Furthermore, the several-kilometre-long section of the river and a very large sloping in the studied river section limit the role of helicoid (helical) movements in the morphological evolution of the riverbed. Therefore we estimated flow velocities and shear stresses using 2D modelling.

2. Study area

Study has been conducted in the catchment of Łomniczka River (sources at 1415 m a.s.l.), in the Karkonosze Mts. (Giant Mts.), the highest part of the Sudetes Mts., SW Poland (Fig. 1). The choice of the Łomniczka River valley for the study was determined by the search for a valley suitable for research. In the Łomniczka valley, we found many places where erosion took place, and also many roots are exposed in different elevations above rivered. In other valleys of the Karkonosze Mountains, there were not so many sites convenient to the study. The choice of the Łomniczka valley allowed for obtaining a large number of dendrochronological dating for modelling, which guaranteed results enabling the reconstruction of hydro morphological parameters. Six study sites were selected in the Łomniczka valley located 700–760 m a.s.l. (Fig. 1). The study area has a cold, mountainous climate with average annual precipitation of 1150–1350 mm (Kasprzak, 2010). It belongs to the lower montane vegetation belt. It is the natural habitat of mixed forests with common beech (*Fagus sylvatica*) and silver fir (*Abies alba*), but due to forest management, Norway spruces (*Picea abies*) are common.

The bedrock of the Łomniczka catchment is composed mainly of granite. Numerous debris flow tracks of diverse age developed in the highest elevations' (968–1370 m a.s.l) during intensive rainfalls (Migoń et al., 2002). Many debris flows were active in July 1997, and some in 2001 and 2002. Several, unusually large debris flows also occurred in
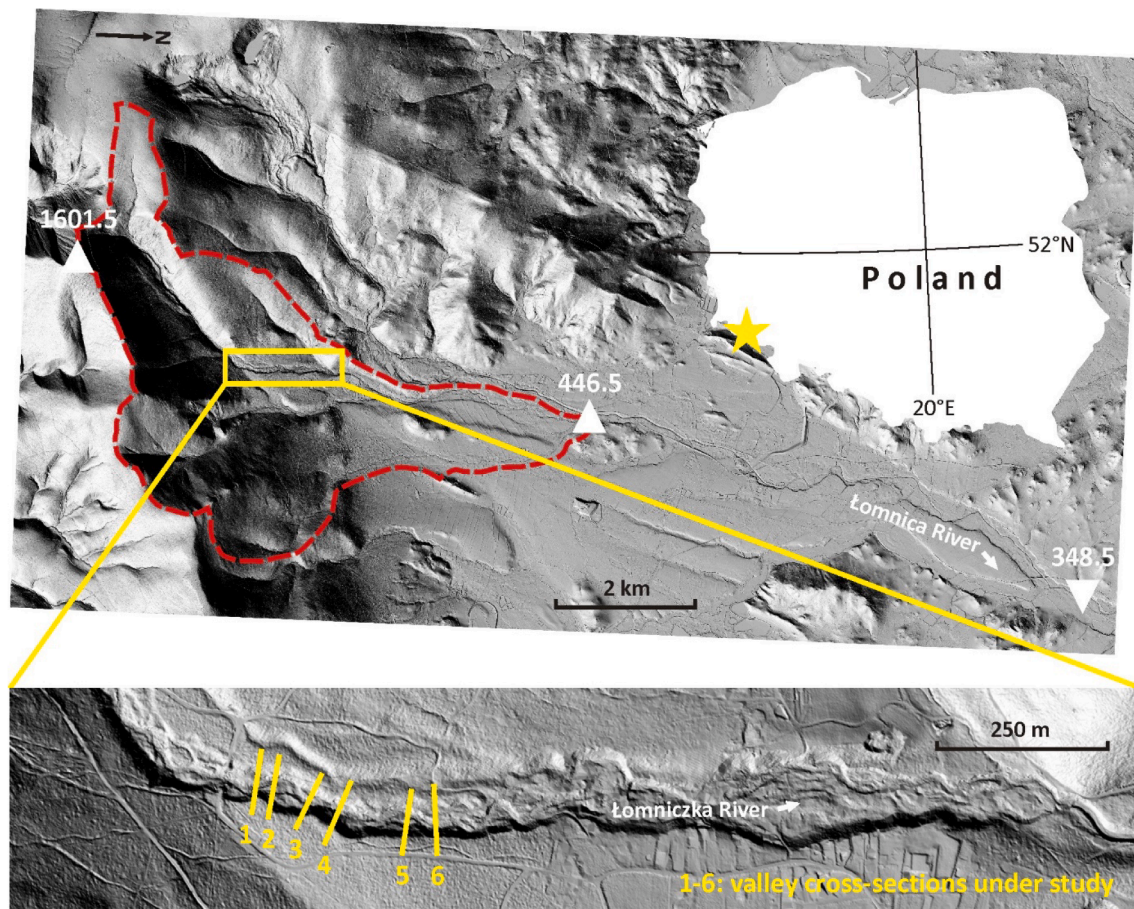
Fig. 1. Location of the study area in SW Poland; location of study sites (valley cross-sections) on the Łomniczka River (Łomniczka basin marked with a dashed line, the highest and the lowest elevation in m a.s.l.) and hydrological gauge on the main Łomnica River (348.5 m a.s.l.).

1964 and 1994. Debris flows in the Łomniczka catchment develop during rainfalls exceeding 100 mm per day and with an intensity of over 10 mm/hour (Parzóch and Dunajski, 2002).

The upper part of the Łomniczka valley has steep slopes, but slopes in the area under study are up to 10%. The bottom of the valley is narrow but flat (Fig. 1). Longitudinal profile of the Łomniczka channel has steps located on bedrock outcrops. The riverbed is often filled with granite boulders up to 1 m in diameter. Tilted and bent trees with exposed roots grow on steep, eroded riverbanks (Fig. 2). In the study reaches, the channel morphology is categorized in the Rosgen Classification system as A1/A2 (Rosgen, 1994). The channel is a single thread a rocky-boulder stream.'

Flood risk on Łomniczka River results from intense precipitation falling on high valley and channel gradients in the upper parts of the catchment, leading to high water velocities and flooding. The most severe floods occur in summer and the entire catchment of Łomnica, main river to Łomniczka, is classified as highly endangered by floods and erosion (Kasprzak, 2010). Łomniczka is the most dangerous stream in this area and causes flood hazard in the whole of the Łomnica catchment.

The nearest stream gauge is located on the Łomnica river (Fig. 1), 4.1–5.0 km downstream from study sites. Gauge provides data since 1959, and the highest hourly discharge was recorded on 07. 07. 1997 (14:00): 146 $m^3 s^{-1}$. In the Łomnica catchment (118 km^2), this equals a large runoff of 1237 $dm^3 s^{-1} km^{-2}$. The second-largest flood occurred on 02. 08. 1977 with a maximum discharge of 118 m3 s-1 at the Łomnica gauge. Large floods also occurred in 1981 and 2002 (96.5 $m^3 s^{-1}$ and 71.4 $m^3 s^{-1}$, respectively) (Fig. 3). Łomniczka River poses the most significant flood hazard in the whole of the Łomnica catchment.

However, hydrological data obtained from the gauge located downstream on the main river are insufficient to estimate flood hazards and provide flood protection in the Łomniczka valley.

3. Methods of the study

3.1. Dendrochronological indication of floods and related bank erosion

The six sampling sites are located in the cross-sections of Łomniczka valley (Fig. 1), where the largest number of exposed roots of Norway spruce was found. In each site, we sampled the thickest roots of one selected tree from eroded banks and at different heights above the riverbed. The lateral distance between roots at one site did not exceed 1.5 m. In total, 28 samples from exposed and injured roots (discs) were collected with a handsaw. At site 1 we collected five root samples, site 2: four samples, site 3: eight samples, site 4: two samples; site 5: five samples and at site 6: four samples. For each study sites (valley cross-sections), we prepared a topographic profile, and we measured the elevation of sampled roots above the bottom of the riverbed with precise geodetic GPS (SinoGNSS). We also measured the distance between the eroded riverbank and sampled parts of exposed roots.

Additionally, we sampled cores from stems of the same Norway spruce trees from which roots were collected. One tree was sampled per study site, and two cores were taken per a tree (a total of 6 trees and 12 cores). Cores were taken with a standard increment borer, parallel to the direction of stem tilting towards river channel and perpendicularly to the direction of flow in the channel. One core was sampled on the bank side of each tree and the other from the opposite, channel side. Additionally, ten reference trees, undisturbed by bank erosion, with straight
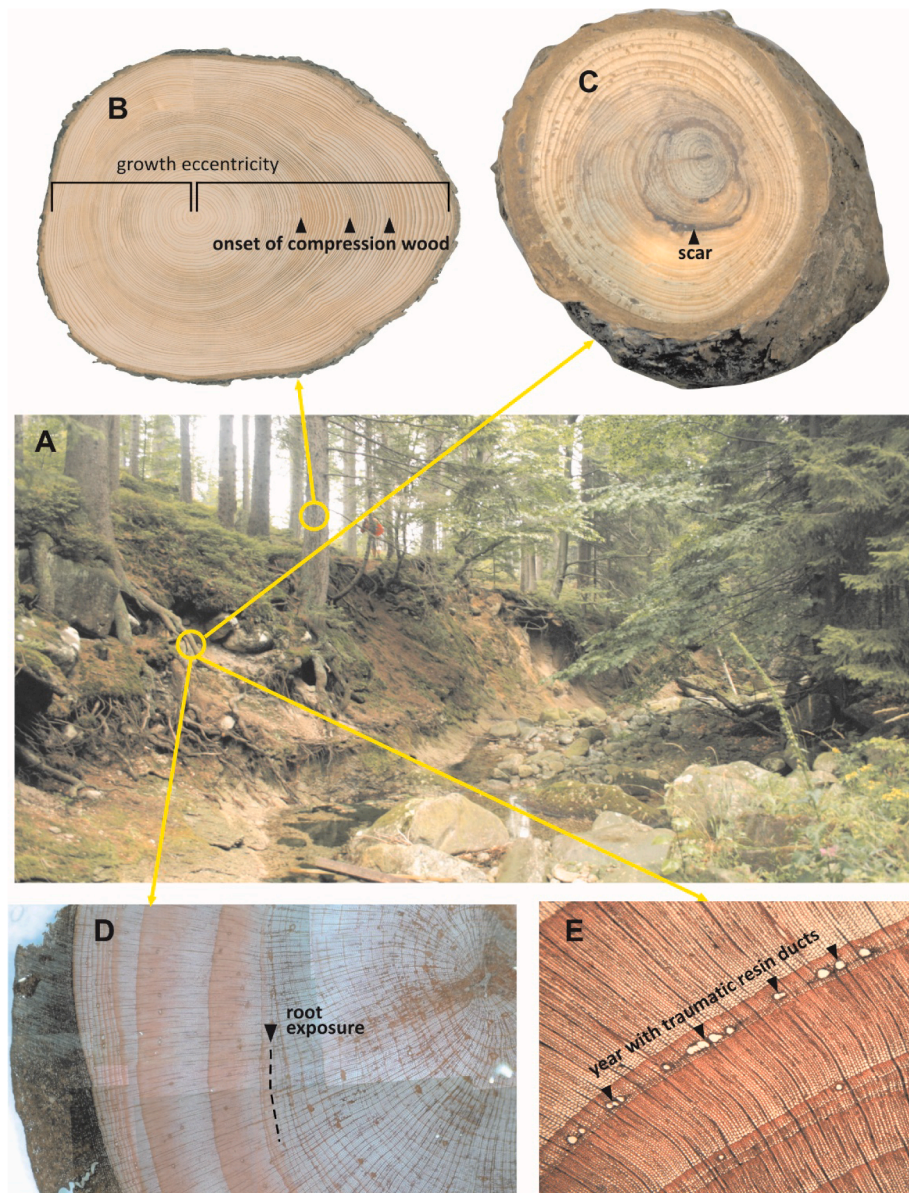
Fig. 2. Exposed tree roots and tilted tree stems on the eroded bank of the Łomniczka River (A). Growth eccentricity and reaction wood on a cross-section of a stem of Norway spruce (B). Scar on a cross-section of a root of Norway spruce (C). Exposure from under soil cover recorded in wood anatomy of a root of Norway spruce (on cross-section, microsection) (D). Traumatic resin ducts on a cross-section (microsection) of Norway spruce root (E).

stems, were sampled on adjacent Łomniczka valley floor.

In the wood of sampled roots, we dated sudden decreases of cell lumen on root cross-sections (Gärtner, 2007) developed due to floods which certainly caused bank erosion at study sites. This growth disturbance records root exposure from under the soil cover by erosion. In sampled cores, we dated reaction wood (i.e. compression wood) and eccentric tree rings developed due to stem tilting by erosion which undermine riverbanks where trees grow (Malik, 2006). We also dated disturbances which develop due to floods but do not prove that erosion occurred at study sites: traumatic resin ducts and scars in roots (Bollschweiler et al., 2008a; Bollschweiler et al., 2008b). Both features record injuries of roots by debris transported by flood. We included only scars and traumatic resin ducts, which occurred after the exposure of a root from under soil cover, when it was certainly affected by floods.

Detailed wood anatomy of roots was analysed on microscopic specimens prepared with GLS microtome (method by Gärtner and Schweingruber, 2013) (Fig. 2). We used WinCell software to date sudden decreases of cell lumens recording root exposure by bank erosion. This

kind of software is commonly used for dating root exposure (Gärtner, 2007), there are no other alternatives so far. We also dated scars and traumatic resin ducts visible. Dating calendar age of wood disturbances was done by counting the number of rings formed after root exposure or injury.

Cores collected from trees were glued into wooden holders and sanded to reveal wood structure. Tree-ring widths were measured using LinTab equipment. Based on ring widths, we have calculated the following indicators of eccentric growth (Fig. 2): per cent index and its yearly variation (method by Wistuba et al., 2013 modified from upslope-downslope to channel-bank stem tilting). This method was chosen for the per cent index and its yearly variation because it is dedicated to analyses of geomorphic processes. Other eccentricity indexes are used for other environmental processes. For example, an index developed by Casteller et al., 2007 is used for avalanche dating. Index described by Burkhalter is commonly used for wind reconstruction (Schweingruber, 1996). Using the method developed by Wistuba et al., 2013 guaranteed obtaining the most precise floods and bank erosion dating.
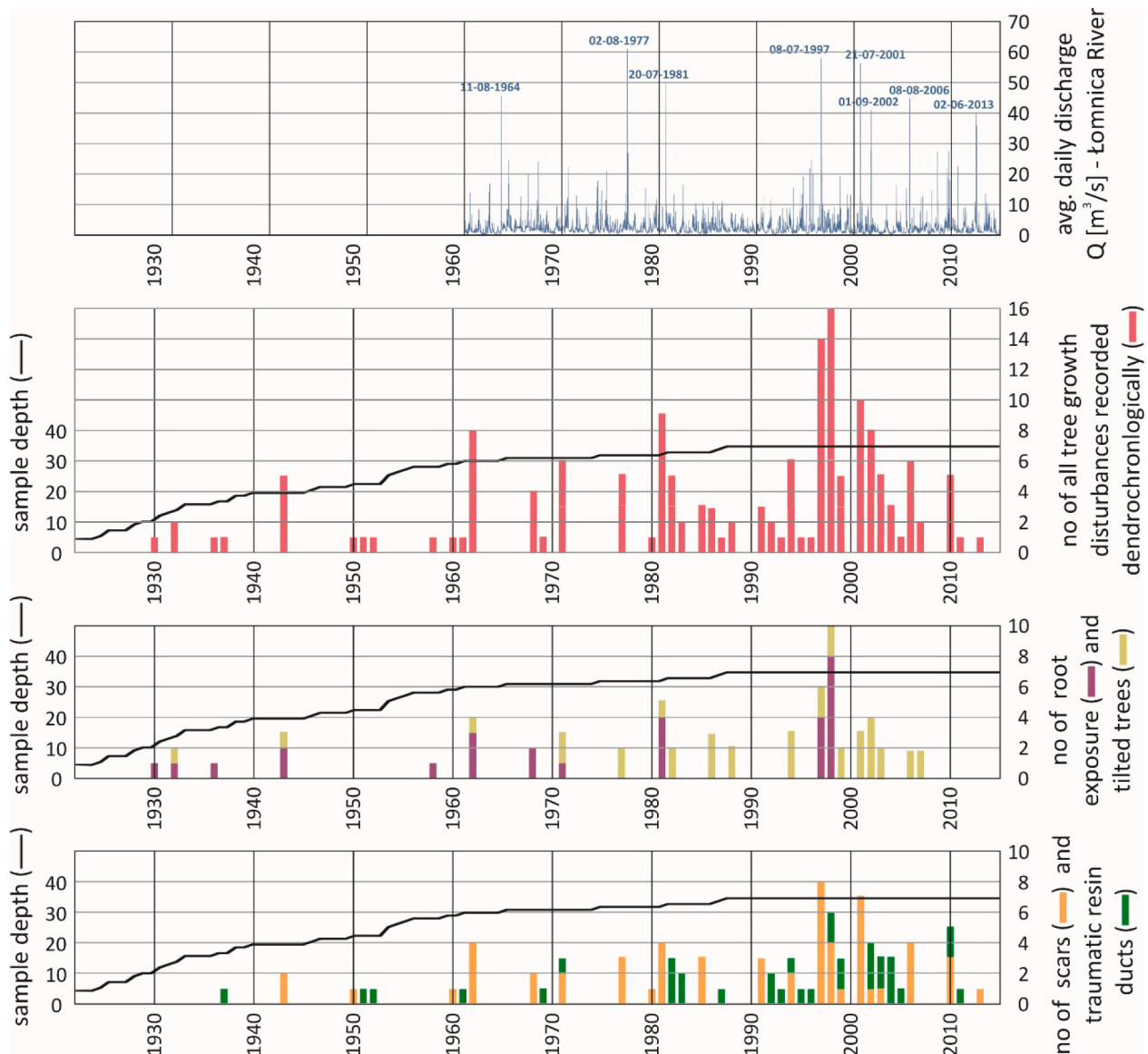
Fig. 3. Average daily discharges at the hydrological gauge on Łomnica River compared with results of dendrochronological dating (all dated growth disturbances and growth disturbances divided into those recording floods and erosion: root exposure and stem tilting, as well as those recording floods but not erosion: root injury).

Results from reference trees (a total of average and standard variation of yearly variations in all tree rings in all reference trees) were used as thresholds in dating events of stem tilting (Wistuba et al., 2013). A 51.08% reference threshold was established for dating events of eccentricity caused by stem tilting in the channel direction.

In each core, we also dated the onset of compression wood (Fig. 2) which was analysed visually, under the binocular microscope.

Compression wood was identified based on thicker cell walls and smaller cell lumens, making it look darker than normal wood (Yumoto et al., 1983). Identification of compression wood, if necessary, was also aided by analysis of microsections under a transmitted light microscope. Microsections were prepared using a core microtome (Gärtner and Nievergelt, 2010).

3.2. Estimation of hydrodynamic parameters

We compared results on floods and related bank erosion obtained from wood anatomy and tree-rings with hydrological record from the closest gauge on the Łomnica River (Fig. 3).

Dendrochronological data were analysed in two groups: disturbances recording bank erosion during floods (root exposure and stem tilting) and disturbances recording floods but not bank erosion (root injuries). We used the measured elevation of sampled roots over channel bed and their distance from eroded riverbanks to estimate water levels during dated flood and erosion events, and minimal rates of bank erosion. This parameters were a basis for further analyses of hydrodynamics parameters.

We used the water levels estimated based on tree roots to quantify the following hydrodynamic parameters: discharges, mean flow velocity and shear stress during specific dated floods. We could not extrapolate the data from the closest hydrological gauge as it is not only located too far from study sites, but it is also located on the main river, not on Łomniczka River. Moreover, we could not use data from gauges in the similar, adjacent catchments (hydrological analogy method). Hydrological conditions in the mountainous area under study are too different, even in neighbouring catchments. Therefore, we used two empirical formulas to calculate discharges during individual floods. The basic calculation was done with the formula by Manning (1891):

$v = 1/n \cdot R_h^{(2/3)} \cdot S^{1/2}$;

$Q = 1/n \cdot A \cdot R_h^{(2/3)} \cdot S^{1/2}$; where: v – water velocity, Q – discharge, n – Manning n value, A – cross-sectional area, S – water surface slope, Rh – hydraulic radius or resistance radius.

The Manning formula is commonly used for discharges calculation, and it is also adopted for different types of software. Discharges obtained with the formula by Manning were used for further calculation in 2D modelling software. However, the results of this calculation were checked with the use of formula by Matakiewicz (1905):

$V = 35.4 \cdot R_h^{0.7} \cdot I^m$; where: v – cross-sectional average velocity, R_h – hydraulic radius, I – slope of the hydraulic grade line, m – exponent related to channel gradient and type of channel, here calculated as follows: m = 0,493 – 2I.

The formula by Matakiewicz was developed particularly for mountain rivers, to calculate maximum discharge s and average water velocities in riverbeds of unsteady and rapid streams with numerous bedrock outcrops and boulders.

We calculated water levels in m a.s.l. and corresponding discharges in the Flow Estimator application, a uniform, steady open channel flow calculator for Quantum GIS 2.18 which applied the formula by Manning. For this purpose, we developed a Digital Elevation Model (1 m × 1 m DEM resolution) for the section of Łomniczka River valley under study. We used LiDAR data from 2012 provided by Central Agency of Geodetic and Cartographic Documentation CODGiK, Poland. We used DEM to calculate water levels along with corresponding discharges in valley cross-sections selected as study sites. Next, we calculated water flow depths, water velocities and shear stress values using Mike 21C software. We identified coefficients of water flow resistance for each study site (Manning n unit: $m^{1/3}/s$, range: 0,045–0,070). We used coefficients in further calculations of hydrodynamic parameters in Mike 21C 2D model. Mike 21C is used for 2D modelling of river morphology; C means "Curvilinear" in reference to the computational mesh. This mesh conforms very precisely to the shape of the curvature of the trough, compared to the flexible mesh (Mike 21, CCHE 2D). In the case of the Mike 21C 2D, we have the option of obtaining total shear stress and skin shear stress results. Skin shear stress allows us to determine the riverbed and riverbank erosion conditions. A separate hydrograph of hourly flows and water levels was prepared for each studied cross-section of the Łomniczka valley in Mike 21C software. We included the range of flows from 1 m^3/s up to the value of the maximum peak flow. The duration of the flow was set at 12 h, including the peak flow lasting at least 2 h. The hydrographs of discharges and water levels at individual study sites (valley cross-sections) during indicated floods were used to determine the boundary conditions in Mike 21C model. Next, a curvilinear grid was developed for the 900-m long part of the Łomniczka River. We used a 1980 × 19 grid size (2.5 m × 5 m spatial resolution) (Fig. 4A).

Lines of the curvilinear grid run along riverbanks which provided better flow resolution near the borders compared to a rectilinear grid. The Manning roughness coefficient of the river bottom and banks was also determined from an orthoimage and field mapping. We decided that accurate field measurement will be the basis for determining the Manning roughness coefficient. Although orthoimages were only the background for the field research, they allowed obtaining general information on the Łomniczka River valley topography and the riverbed roughness. The roughness coefficients were considered in spatial classes (0,045–0,070). The eddy viscosity of 0.40 was calculated using a formula by Smagorinsky (1963). Next, we imported the height from DEM into the curvilinear grid; we created a bathymetric model enabling the assessment of curvilinear motion, water velocities in different directions, water depth and shear stresses (Fig. 4B). The curvilinear grid model allows performing calculations showing the distribution of curvilinear velocities. The current curvature is calculated as the vector product of velocity and acceleration. Thus, the curvilinear mesh makes it possible to calculate curvilinear velocities in the simulation of hydrodynamics. In addition to calculating the velocity in the mainstream axis, it is possible to calculate flow velocity with directions and turns other

than parallel to the current line - transverse, diagonal or opposite. The model of the variation of initial water surface elevation was developed based on DEM from LiDAR and geodetic field measurements of underwater riverbed morphology. The longitudinal slope changed locally from 63 to 98‰ (Fig. 4C).

4. Results

We dated 120 growth disturbances in 28 tree root samples collected from study sites along the Łomniczka River, including 28 disturbances by exposure from under the soil cover, 58 scars, and 34 traumatic resin duct disturbances (Fig. 3). In 6 tree stems, we dated 37 growth disturbances developed due to stem tilting (tree-ring eccentricity and compression wood) (Fig. 3). In 1943, 1962, 1971, 1981, 1986, 1994, 1997, 1998, 2001, 2002 (Fig. 3, Table 1) we found more than two growth disturbances recording floods and bank erosion (root exposure and tree tilting) per year. In 1962, 1971, 1981, 1986, 1991, 1994, 1997, 1998, 1999, 2001, 2002, 2003, 2006, 2010 (Fig. 3, Table 2) we found more than two growth disturbances recording only floods, but not bank erosion (root injury) per year.

Two and less growth disturbances recording floods and erosion per year were dated in 1930, 1932, 1936, 1958, 1968, 1977, 1982, 1988, 1999, 2003, 2006, 2007 (Fig. 3, Table 1), while two and less disturbances recording only floods, but not erosion, occurred in 1937, 1943, 1950, 1951, 1952, 1960, 1961, 1968, 1969, 1980, 1983, 1987, 1992, 1993, 1995, 1996, 2005, 2011, 2013 (Fig. 3, Table 2).

The comparison of dendrochronological results with hydrological data (Fig. 3) shows that majority of events recorded by trees match years with floods recorded at the gauge, including 1981, 1997, 2001, 2002–2003 (flood in September 2002, after the growing season, recorded by trees in 2003), 2006–2007 (flood in August 2006, at the end of the growing season, recorded by trees in 2006 and 2007), 2010 and 2013.

Measurements of the distance of sampled roots from the eroded riverbanks and their elevation above riverbed show that during floods with erosion in 1930 (site 4), 1932 (site 1), 1943 (site 2), 1981 (site 1) and 1997 (site 6) roots were exposed relatively high. Distances between the exposed roots and the riverbed were also significant (Tables 1, 3).

Measurements indicate that rates of bank erosion at study sites in listed years could have been quite significant. Results also show that the rest of dated floods did not cause considerable erosion at study sites, or the erosion occurred but was not recorded by trees. In some years (1977, 1986, 1988, 1994, 2001–2003, 2006–2007) erosion was identified only from stem tilting. Therefore, during these floods erosion occurred, but it did not expose any roots.

Both floods which, according to tree-ring data, caused bank erosion (1930, 1932, 1936, 1943, 1958, 1962, 1968, 1971, 1981 and 1997) and floods for which we did not find dendrochronological proofs of erosion (1950, 1960, 1977, 1980, 1985, 1991, 1994, 1999, 2001, 2002, 2003, 2006, 2010 and 2013) were included in the estimation of hydrodynamic parameters. Estimated maximum discharges derived from formulas by Matakiewicz and Manning (Tables 4 and 5) for floods recorded at individual sites varied, from small (only 3.8 m^3 s^{-1}) to much larger (up to 106,7 m^3 s^{-1}). Calculations of discharges from formulas by Matakiewicz and Manning are generally similar in the same cross-sections, but they can differ for smaller floods (Tables 4, 5).

For example, the discharge in 1998 (site 3) estimated from the Matakiewicz formula was 11.5 m^3 s^{-1} while the estimated from Manning formula was smaller by over a half: 4,7 m^3 s^{-1}. Calculations with both formulas showed that the smallest discharges probably occurred during floods in 1998, 2001 and 2010 (site 5): 3.8–6.1 m^3 s^{-1} (Tables 4, 5). On the other hand, the highest discharges probably occurred during the 1997 flood (site 6): 106.7 m^3 s^{-1} according to Matakiewicz formula and 98.1 m^3 s^{-1} according to formula by Manning formula (Tables 4, 5).

The highest discharges among dated events which certainly caused erosion, were estimated for floods in 1932 and 1943 (84.1–98.3 m^3 s^{-1}
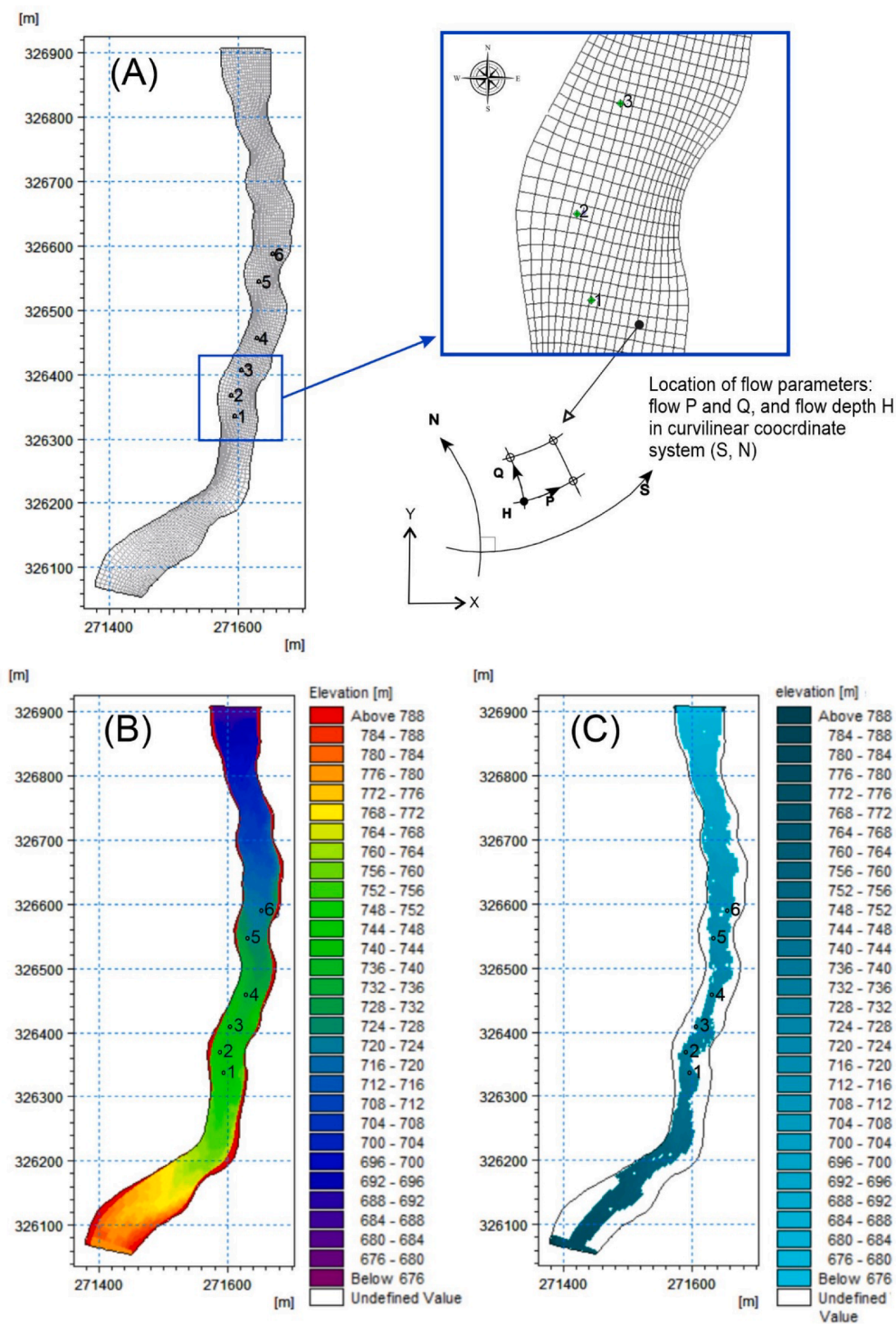
Fig. 4. Data for simulation in Mike 21C model: the curvilinear grid of Łomniczka River (A), bathymetry model from DEM (riverbed and terraces) (B) and initial (water) surface elevation model for riverbed (C) with study sites marked (1–6). The stream is flowing from North (top of page) to South (bottom of page).

Table 1

Dating floods with erosion recorded by tree root exposure and stem tilting (growth eccentricity and compression wood).

Study site / sampled tree	Sampled root	Root elevation over riverbed [cm]	Root distance from riverbank [cm]	Dated root exposure	Dated stem tilting
1	1–1	180	100	1981	1981,
	1–2	190	90	1932	1982,
	1–3	180	100	1981	1986,
	1–4	180	100	1981	1988,
	1–5	180	100	1981	2002, 2003
2	2–1	180	60	1943	1971,
	2–2	110	20	1968	1977,
	2–3	180	120	1943	1982,
	2–4	110	30	1968	1986, 2002
3	3–1	80	60	1971	1962,
	3–2	100	40	1962	1971,
	3–3	80	60	1958	1977,
	3–4	60	120	1998	1986,
	3–5	60	110	1998	1994,
	3–6	60	120	1998	1997,
	3–7	100	50	1962	2001,
	3–8	100	40	1962	2003, 2006
4	4–1	130	100	1930	1932,
	4–2	90	60	1936	1943, 1988
5	5–1	80	30	1998	1994,
	5–2	45	10	1998	1998,
	5–3	80	40	1998	1999,
	5–4	80	30	1998	2001,
	5–5	45	40	1998	2002, 2005
6	6–1	220	120	1997	1994,
	6–2	140	70	1997	1997,
	6–3	200	110	1997	1998,
	6–4	220	100	1997	1999, 2001, 2002, 2005, 2006

Table 2

Dating floods without erosion, recorded only by root injury (scars and traumatic resin ducts).

Study site	Sampled root	Dated scars	Dated traumatic resin ducts
1	1–1	1981, 1991, 1997, 2001	1992, 1994
	1–2	1991, 1997, 2001	1992
	1–3	1997,	
	1–4	1981, 1991, 1997	1982, 1983, 1993, 1998
	1–5	1981	1982
2	2–1	1977	
	2–2	1968, 1980	1969
	2–3	1977	
	2–4	1968	
3	3–1	1971, 1985	
	3–2	1962, 1971, 1985, 1994	1971, 1987
	3–3	1977, 1962, 1985, 1994, 2001, 2006	1995, 1996
	3–4	1998, 2006	1999
	3–5	2006	
	3–6	1998	
	3–7	1962	
	3–8	1962, 1981	1982, 1983
4	4–1	1943	1937
	4–2	1943, 1950, 1960	1951, 1952, 1961
5	5–1	1998	
	5–2	2003	2004, 2005
	5–3	1999, 2002	2003, 2004
	5–4	2001, 2010, 2013	
	5–5	1998, 2001, 2010	2002, 2003, 2004
6	6–1	1997	1998, 1999
	6–2	1997, 2006, 2010	2011
	6–3	1997, 2001	2002, 2010
	6–4	1997, 2001	2002, 2010

Table 3

Rates of bank erosion calculated for individual past floods.

Study site	Dated flood	Bank erosion annual rates based on wood anatomy of roots [cm]
1	1932	90
	1981	100
2	1943	60
	1968	20
3	1958	60
	1962	40–50
	1971	60
	1998	110–120
4	1930	100
	1936	60
5	1998	10–60
6	1997	70–120

and 57.9–70.6 m³ s⁻¹ respectively) (Table 4). Among events for which no proofs of erosion were found, the highest discharges were estimated for floods in 1997 and 2001 (80.4–106.7 m³ s⁻¹) (Table 5). However, dendrochronological record of the 1997 flood is unique. Erosion was confirmed at site 6 at an elevation of 70–120 cm above the riverbed (Table 4), but at the same time flooding (without erosion) was confirmed in the same study site at an elevation of 140–200 cm (Table 5). It indicates that the maximum flow estimated from tree-ring record of a flood with erosion (9.18–35.08 m³ s⁻¹) is underestimated, and that the water level during this flood reached up to 220 cm above the riverbed (Table 4). With such high water level, the discharge values of 80.4–106.7 m³ s⁻¹ should be used for further estimation of flow velocity and shear stress values during the 1997 flood.

In determining flow velocity and shear stress values during specific floods with a 2D model (Tables 4, 5), we assumed that tree roots were exposed or wounded during the largest flood in each dated calendar year. This is the most likely scenario, but it cannot be ruled out that the roots were exposed during lower flows. Values of flow velocity estimated at individual study sites vary from as low as 0.17–0.2 m/s (site 3 in 1958, 1962, and 1998), to very high: 4.59 m/s (site 4 in 1930) (Table 4, 5). Shear stress values estimated directly for eroded banks where tree roots were sampled (Tables 4, 5) vary from low: 81.2 N/m² (site 3 in 1962) up to 510,3N/m2 (site 2: 1943 and 1977) and 469.1 N/m² (site 6: 1997). In general, the highest values of shear stress during events of bank erosion were found for site 2, where it reached 510,3N/m² in 1943 and site 4, where it was 344.3 N/m² in 1930. Figs. 5 and 6

present examples of results on water velocity and shear stress calculated with a 2D model for two selected floods recorded in tree rings.

5. Discussion

5.1. The accuracy and limitations of dendrochronological dating of floods and bank erosion

The majority of flood and erosion events recorded in the wood of trees under analysis match with high discharges recorded at the hydrological gauge. This similarity demonstrates the high accuracy of the dendrochronological dating. In some cases (e.g. 1981 and 2010) growth disturbances were recorded partly in the year when flood and bank erosion occurred and partly in the next year. Environmental factors affecting wood anatomy of trees are often recorded a year later after a disturbing event occurred. This particularly concerns flood and erosion occurring at the end, or after the growing season, e.g. in September (Bodoque et al., 2005; Bollati et al., 2012; Malik and Wistuba, 2012).

Table 4
Hydrodynamic parameters reconstructed based on tree-ring data for floods with confirmed bank erosion.

Study site	Root elevation over riverbed [cm]	Elevation [m a. s.l.]	Event of flood and erosion	Hydrodynamic parameters from Matakiewicz formula		Hydrodynamic parameters from Manning formula		Erosion parameters for individual cells tangent to riverbanks on a 2D model			
				Discharge [m³ s⁻¹]	Mean velocity [m/s]	Peak discharge [m³ s⁻¹]	Mean velocity [m/s]	Mean velocity [m/s]	Direction X velocity [m/s]	Direction Y velocity [m/s]	Total shear stress [N/m²]
1	180	741.99	1981	71.4	4.34	75.8	4.14	3.46	1.54	2.89	145.2
	190	742.09	1932	98.3	5.11	84.1	4.26	3.51	2.05	2.88	169.5
2	180	739.48	1943	70.6	6.38	57.9	3.72	1.64	1.47	0.72	510.3
	110	738.78	1968	27.7	4.82	19.2	2.71	0.89	0.73	0.50	331.6
3	80	735.81	1971	17.1	4.35	9.9	2.11	0.44	0.43	0.09	115.3
	40–50	735.41–735.51	1962	4.3–5.1	1.55–1.68	2.11–3.32	1.42–1.56	0.17–0,18	0.15–0.01	0.10–0.01	81.2–86.7
	60	735.61	1958	11.5	3.87	4.7	1.67	0.20	0.14	0.08	109.0
	60	735.61	1998	11.5	3.87	4.7	1.67	0.20	0.14	0.08	109.0
4	130	729.9	1930	44.8	3.49	47.0	3.43	4.59	4.56	0.15	344.3
	60	729.2	1936	9.11	2.26	8.40	1.88	2.22	1.50	−0.06	144.3
5	45–80	719.07–719.41	1998	3.8–6.1	2.83–3.23	3.9–18.1	1.32–2.22	1.85–2.64	1.84–2.64	−0.01–0.2	148.6–205.2
6	70–120	714.94–715.44	1997	9.18–35.08	2.22–3.11	7.04–29.01	1.98–2.78	2.29–3.83	2,57–3.68	−0.54–1.07	213.2–283.9

Table 5
Hydrodynamic parameters reconstructed based on tree-ring data for floods without confirmed bank erosion.

Study site	Root elevation over riverbed [cm]	Elevation [m a. s.l.]	Event of flood	Hydrodynamic parameters from Matakiewicz formula		Hydrodynamic parameters from Manning formula		Erosion parameters for individual cells tangent to riverbanks on a 2D model			
				Discharge [m³ s⁻¹]	Mean velocity [m/s]	Peak discharge [m³ s⁻¹]	Mean velocity [m/s]	Mean velocity [m/s]	Direction X velocity [m/s]	Direction Y velocity [m/s]	Total shear stress [N/m²]
1	180–190	741.99–742.09	1991	71.4–98.3	4.34–5.11	75.8–84.1	4.14–4.26	3.46–3.51	1.54–2.05	2.89–2.89	145.2–169.5
	180–190	741.99–742.09	1997	71.4–98.3	4.34–5.11	75.8–84.1	4.14–4.26	3.46–3.51	1.54–2.05	2.89–2.89	145.2–169.5
	180–190	741.99–742.09	2001	71.4–98.3	4.34–5.11	75.8–84.1	4.14–4.26	3.46–3.51	1.54–2.05	2.89–2.89	145.2–169.5
2	110	738.78	1968	27.7	4.82	19.2	2.71	0.89	0.73	0.50	331.6
	180	739.48	1977	70.6	6.38	57.9	3.72	1.64	1.47	0.72	510.3
	110	738.78	1980	27.7	4.82	19.2	2.71	0.89	0.73	0.50	331.6
3	80–100	735.81–736.01	1962	17.1–22.3	4.35–4.41	9.9–26.1	2.11–2.4	0.44–2.72	0.43–2.71	0.08–0.09	115.3–296.4
	80–100	735.81–736.01	1971	17.1–22.3	4.35–4.41	9.9–26.1	2.11–2.4	0.44–2.72	0.43–2.71	0.08–0.09	115.3–296.4
	80	735.81	1977	17.1	4.35	9.9	2.11	0.44	0.43	0.09	115.3
	80–100	735.81–736.01	1985	17.1–22.3	4.35–4.41	9.9–26.1	2.11–2.4	0.44–2.72	0.43–2.71	0.08–0.09	115.3–296.4
	80–100	735.81–736.01	1994	17.1–22.3	4.35–4.41	9.9–26.1	2.11–2.4	0.44–2.72	0.43–2.71	0.08–0.09	115.3–296.4
	60	735.61	1998	11.5	3.87	4.7	1.67	0.20	0.14	0.08	109.0
	80	735.81	2001	17.1	4.35	9.9	2.11	0.44	0.43	0.09	115.3
	60–80	735.61–735.81	2006	11.5–17.1	3.87–4.35	4.7–9.9	1.67–2.11	0.20–0.44	0.14–0.43	0.08–0.09	109.0–115.3
4	90–130	729.9–730.3	1943	28.4–4.8	2.9–3.49	23.5–47.0	2.79–3.43	3.57–4.59	3.57–4.56	−0.02–0.15	234.0–344.3
	90	729.5	1950	28.4	2.9	23.5	2.79	3.57	3.57	−0.02	234.0
	90	729.5	1960	28.4	2.9	23.5	2.79	3.57	3.57	−0.02	234.0
5	45–80	719.07–719.41	1998	3.8–6.1	2.83–3.23	3.9–18.1	1.32–2.22	1.85–2.64	1.84–2.64	−0.01–0.2	148.6–205.2
	80	719.41	1999	6.1	3.23	18.1	2.22	2.64	2.64	−0.01	205.2
	45–80	719.41	2001	3.8–6.1	2.83–3.23	3.9–18.1	1.32–2.22	1.85–2.64	1.84–2.64	−0.01–0.2	148.6–205.2
	80	719.41	2002	6.1	3.23	18.1	2.22	2.64	2.64	−0.01	205.2
	45	719.07	2003	3.8	2.83	3.9	1.32	1.85	1.84	0.2	148.6
	45–80	719.41	2010	3.8–6.1	2.83–3.23	3.9–18.1	1.32–2.22	1.85–2.64	1.84–2.64	−0.01–0.2	148.6–205.2
	80	719.41	2013	6.1	3.23	18.1	2.22	2.64	2.64	−0.01	205.2
6	140–220	715.64–716.44	1997	45.7–106.7	5.80–5.89	43.7–98.1	3.19–4.53	4.25–5.17	4.19–4.83	−1.39–1.86	285.6–469.1
	200–220	716.24–716.44	2001	80.4–106.7	5.31–5.89	95.2–98.1	4.23–4.53	4.01–5.02	3.78–4.11	−1.23–1.35	469.1–579
	140	715.64	2006	45.7	5.80	43.7	3.19	4.25	4.19	−1.39	285.6
	140	715.64	2010	45.7	5.80	43.7	3.19	4.25	4.19	−1.39	285.6

The delayed reaction of trees also occurs after their stems are tilted on eroded riverbanks. Thus, development of compression wood and eccentric tree rings can start in the year of tilting or next year, and it can last for several years after the event which caused stem tilting, e.g. flood and erosion in 1981 (Fig. 3). Development of traumatic resin ducts also can occur in the year of wounding, next year or few years after wounding by debris transported in a flood, e.g. 1950, 1991.

In some cases, increased number of dendrochronological disturbances recorded in studied trees does not match precisely with daily discharges recorded at the gauge (e.g. 1964 and 1977: highest discharges recorded at gauge with poor record in wood anatomy) (Fig. 3). These differences may result from the fact that each flood partially destroys the dendrochronological record of all previous floods by damaging already exposed roots and undermined trees. This is probably the reason why the oldest flood recorded at the gauge, e.g. 1964 and 1977, have poor tree-ring record (Fig. 3). This means that older floods and erosion episodes are not often recorded in the wood of trees growing in river valleys now. Older floods can only be recorded in more stable sections of riverbeds, in sections where river migrate laterally and erosion episodes appear relatively often, older flood and erosion episodes will be absent, mainly because trees that recorded these episodes were undercut during a flood and fallen to the riverbed.

There are also some events recorded in trees which do not match with significant daily discharges measured at the gauge (1962, 1985–1991, 1994, 1998, 2000). This may result from the occurrence of flood events covering only the area of the Łomniczka River catchment, i. e. caused by precipitation events of limited extent like summer downpours, and too small to significantly influence hydrological records of
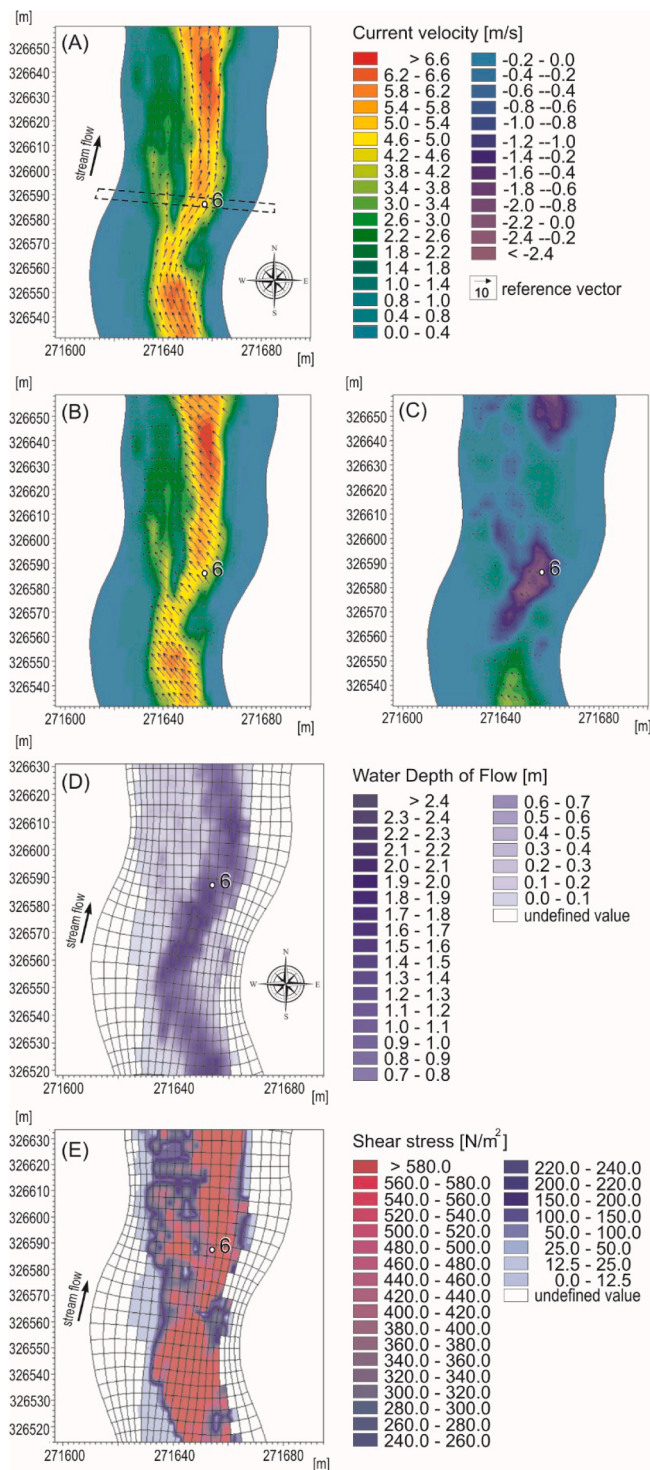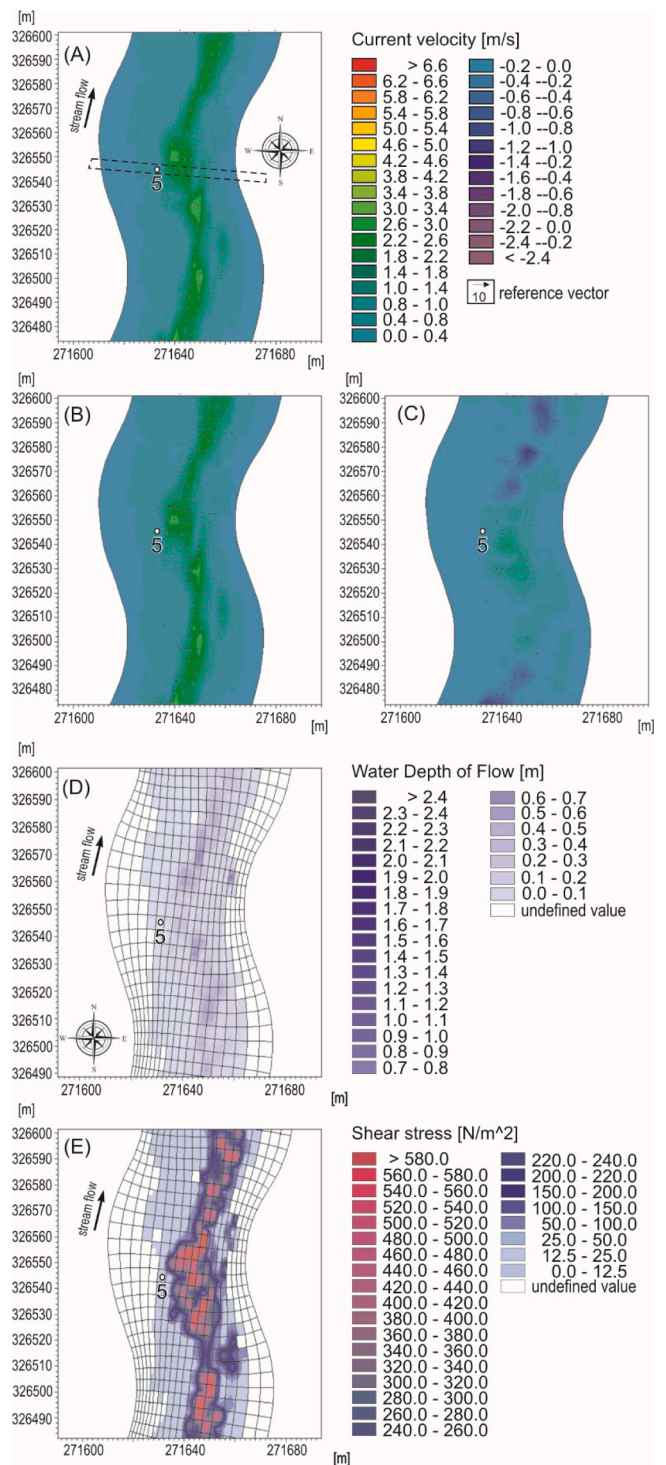
Fig. 5. Hydrodynamic parameters mapped in Mike 21C for study site 6 during the reconstructed discharge peak (98.1 m³s) of Łomniczka River in 1997, i.e. 2D maps of current velocity and velocity vectors (A), current velocity in the X direction (B), current velocity in the Y direction (C), water flow depth (D) and shear stress (E).

Fig. 6. Hydrodynamic parameters mapped in Mike 21C for study site 5 during the reconstructed discharge peak (3.9 m³s) of Łomniczka River in 2001, i.e. 2D maps of current velocity and velocity vectors (A), current velocity in the X direction (B), current velocity in the Y direction (C), water flow depth (D) and shear stress (E).

the main Łomnica River, where the gauge is located (Fig. 1). Precipitation in mountain ranges is very varied and often occurs locally. Therefore, flood episodes are usually recorded on non-distant watercourses flowing in the upper parts of the catchment area, while in larger rivers located not far away, these episodes are not recorded but are only recorded to a minor extent.

The high accuracy of dendrochronological dating can also be demonstrated by a comparison between the size of individual floods recorded at the hydrological gauge and the number of dated growth disturbances. Particularly large floods, like the July 1997 flood (in Poland the so-called Millennium Flood), were recorded by numerous trees growth disturbances. Similarly, major floods in 1981 and 2001 are very well documented in wood anatomy and tree rings. The number of

all dendrochronological disturbances recording floods and erosion is significantly increased since 1980. The particularly increase in the number of growth disturbances dated in studied trees has been found since the mid-1990s (Fig. 3). However, this increase may be apparent and occur only due to the underestimated number of disturbances related to older events. Younger floods can destroy roots with disturbances from previous events and, therefore, erase their dendrochronological record. On the other hand, the number of large floods in the study area has increased significantly since the mid-1990s, which certainly caused more erosion and floods recorded in the wood of the trees (Fig. 3).

The main issue with indication water levels during bank erosion events is the assumption that water flowed at the elevation where roots were exposed. Earlier observations indicate that the roots are exposed at the level where water flows during the flood (Malik and Matyja, 2008). However, roots can also be exposed above the level of flooding. Erosion below the level of roots can undermine riverbank, cause failure of the soil above and expose roots. However, this seems unlikely in the studied case, as roots were often injured at the time of their exposure. Injury can only be explained through the impact of debris transported by flowing water. Therefore, root injury during exposure is evidence of water flowing at least at the elevation of the root. However, the water level could have exceeded root elevation significantly, which makes estimated hydrological parameters underestimated.

In most cases, dendrochronological dating of floods and bank erosion is based on all growth disturbances identified in wood samples (e.g. Šilhán, 2015). Ruiz-Villanueva et al. (2010) reconstructed the timing and frequency of several flash floods using different types of tree growth disturbances. Selection of specific types of growth disturbances is less frequent (e.g. Astrade and Bégin, 1997; Casteller et al., 2015). In the studied case, we have combined dating wood anatomy features in exposed and wounded roots with the dating of growth eccentricity and compression wood in tilted stems. These anatomical features were selected because they undoubtedly result from the erosion of riverbanks. The probability for root exposure on riverbanks and tilting of stems growing on riverbanks towards the channel due to factor other than erosion (e.g. wind for stem tilting) is small.

In our analysis, we did not include some disturbances of wood anatomy often applied in dendrochronological indication of erosion which can be caused not only by erosion but also other environmental factors. We did not include compression wood in roots which can also be developed due to, e.g. biomechanical weathering (Malik et al., 2019). We also omitted dating reductions of tree-ring widths in roots and stems as they can result, e.g. from insect outbreaks (Büntgen et al., 2009; Konter et al., 2015) or air pollution (Jämbäck et al., 1999; Elling et al., 2009; Malik et al., 2012). Local factors, such as insect outbreaks, can even be absent in reference trees sampled close to study trees. Therefore, including ring reductions in indication of erosion can affect the results and cause errors in dating floods and related bank erosion. Growth disturbances applied in dating of selected environmental factor (e.g. flood, erosion, air pollution, etc.) should be carefully selected. Analysing all growth disturbances found in wood samples may cause errors in dating which, sometimes, cannot be prevented even with the use of reference trees.

5.2. The accuracy and potential of dendrochronology and 2D modelling in indication of floods and bank erosion

The risk of errors in conducted tree-ring indication of floods, erosion and their hydrodynamic parameters is particularly high for older events. At the time of older floods, the relief of riverbed in study sites (valley cross-sections) was probably different than today, in particular taking into account bank erosion in years following the dated event. For example, in this study, we estimated very high discharges, flow velocities and shear stress values for floods and erosion in 1930 and 1943 (Tables 4, 5). However, in 1930 and 1943, the riverbed of Łomniczka

could have been different, e.g. it could have been narrower or shallower. Events of erosion which occurred since 1943, could have widened and deepened the riverbed. Therefore, hydrodynamic parameters estimated for older floods but based on contemporary topography can be incorrect.

Hydraulic modelling of floods has been recently based on the use of Digital Elevation Models (DEMs) (Tarekegn et al., 2010; Masood and Takeuchi, 2012). In addition to DEMs, modelling involves data from water gauges, usually located in lower river reaches, not on small mountain rivers. Modelling allows to estimate various hydrodynamic parameters in valleys where hydrological measurements are not conducted (Grimaldi et al., 2013; Jafarzadegan and Merwade, 2017). Such estimations may be incorrect, in particular, if hydrological gauges are distant from area subjected to modelling.

Dendrochronological dating of tree roots, with some above-described restrictions, allows to determine water levels during specific floods (Ballesteros Cánovas et al., 2011). Data on water levels obtained from tree rings can be an input for 2D modelling and can help to improve its accuracy in ungauged area. More accurate results of calculations of flow velocity can be expected from riverbed sections with small roughness and uniform stream gradient because they guarantee better adjustment to requirements of formulas and mathematical models.

Dendrochronological data on flood frequency, data on modelled discharges and flow velocities, as well as on river sections exposed to erosion are a valuable input for designing hydrotechnical facilities, flood protection, urban planning and for local plans of spatial development (de Moel et al., 2009; Neuvel and Van den Brink, 2009). Data on historical floods are also used by water administrations to prepare flood hazard and risk maps (Di Baldassarre et al., 2009). Also dendrochronological analyses can be used to determine areas threatened by floods more accurately. This particularly concerns planning the development in mountain valleys where trees and dendrochronology can help to outline areas potentially subjected to flooding. Then, maps of flood hazard and risk can be developed from water levels and discharges estimated locally from tree rings, rather than based on data from distant hydrological gauges. Therefore, application of dendrochronology should improve the accuracy of flood hazard and risk maps, also taking into account potential locations of infrastructure outside erosion and flooding zones. Thus, dendrochronological analyses of floods and erosion can help to avoid or reduce damages in ungauged mountain areas significantly (Hajdukiewicz et al., 2015).

2D modelling can be applied to estimate conditions of bank erosion during past events indicated from tree rings. In this study, we were able to estimate the hydrodynamic parameters even for floods which occurred before the closest stream gauge was founded in 1959, e.g. for floods in 1932, 1936, 1943 and 1958 (Table 4). For each flood recorded by trees in study sites, we estimated bank erosion, discharge, flow velocity and shear stress. Values of hydrodynamic parameters estimated for floods with no tree-ring evidences of erosion are often much higher than those determined for floods with documented erosion (Tables 4, 5). For example, during floods in 1950, 1960, 1980, 1985, 1991, 1994, 1999, 2001, 2006, 2010 and 2013 shear stress values exceeded 200 N / m^2. Therefore, we can assume that erosion also occurred during these floods, although no record of exposed roots and tilted stems has been found for this years in the samples. During massive floods with high erosion rates, trees that grow on riverbanks fall into stream channels, and erosion episodes are not recorded (Vandekerckhove et al., 2001b; Malik, 2006). Therefore, it is possible that also in the studied case, large floods have fallen trees and destroyed tree-ring record of erosion.

Dendrochronological analyses can yield new, previously unavailable precise information on erosion during historical floods (Dean, 1988). Hydrodynamic parameters estimated with 2D models strongly depend on these dendrochronological input data, mainly through indicated levels of water during events of floods and erosion (Ballesteros Cánovas et al., 2011). On the other hand, the results of modelling depend on the accuracy of calculations which depend on the type of 2D model and included parameters (Horritt and Bates, 2002). According to Hankin

et al. (2019), the use of the 2D model effectively indicates areas susceptible to river erosion and allows to estimate water velocity, shear stress and the susceptibility of the material to erosion (Lane and Ferguson, 2005; Reid et al. 2019). Pasternack et al. (2006), based on the study of mountain rivers, state that the use of 2D models provides very high accuracy compared to field measurements. Pasternack and Senter (2011) and Pasternack and Wyrick (2016) in their studies of flood discharges in steep sections of mountain rivers indicated that the predicted water velocity and shear stress in the 2D model is 95% compatible with the best field estimation method. The 2D model Mike 21C helped us to calculate flood discharges which caused erosion. Precise results were obtained for cells of the model directly tangent to the riverbanks, not only the average value for entire cross-section as commonly used with 1D models or empirical formulas (Horritt and Bates, 2002; Morianou et al., 2016). 2D maps of hydrodynamic parameters (water flow velocity in different directions, water flow depth and shear stress) obtained in this study for the culmination of flood scenarios quite clearly show the possible occurrence of high energy conditions in study sites (valley cross-sections). 2D maps show that maximum flow velocities for grid cells tangent to the riverbanks exceeded the velocity value necessary for even coarse material to be eroded (Clark and Wynn, 2007). It seems that by further analyses, we could also estimate the size of material which was eroded during particular past floods. However, a more detailed study of the structure of eroded riverbanks in individual sites would be necessary.

We applied the curvilinear model for improved accuracy of results. Curvilinear computational grid for the Mike 21C mode is an unstructured grid, adapted to the curvatures of the channel, which allows for more details in the design area. It allows to eliminate details in areas of less hydraulically essential results. According to Morianou et al. (2016), the results obtained with the curvilinear model are more consistent with field measurements than the results of calculations using the rectilinear model. For indicated floods, besides depth-averaged maximum flow velocity values in grid cells, we also obtained maximum flow velocity values parallel to the riverbanks (current velocity in the X direction) and perpendicular to the riverbanks (current velocity in the Y direction) (Fig. 4A). Such results are essential for the assessment of water energy which determines erosion of the banks. For example, for all water levels indicated from tree rings at site 1, the maximum water velocity in the Y direction was dominant (2.88–2.89 ms^{-1}) compared to the maximum water velocity in the X direction (od 1.54 do 2.05 ms^{-1}) (Tables 4, 5). Higher water velocity in the Y direction at individual positions indicates a high possibility for bank erosion. At site 6, on the other hand, for all water levels, values of the maximum flow velocities from the Y direction in the cells tangent to the edge were negative, which indicates a strong turbulence of water flow during floods at this location. In general, it seems that by selecting appropriate dendrochronological techniques and with the use of 2D modelling, it is possible to estimate the conditions of erosion during individual floods, even if they were not recorded at hydrological gauges.

6. Conclusions

Using dendrochronological methods, it is possible to indicate the years of floods when bank erosion occurred and floods when bank erosion was not recorded in small ungauged catchments. It is also possible to estimate the rates of bank erosion at individual sites where bank erosion was recorded in tree rings. Dendrochronology allows to indicate water levels during particular floods which can be used to calculate hydrodynamic parameters. Parameters for floods without recorded bank erosion can be analysed based on scars and traumatic resin ducts. They can be separated from parameters for floods with erosion events recorded as root exposure and stem tilting (reaction wood and tree ring eccentricity). Dendrochronological data, when combined with field measurements of contemporary valley relief, can provide a basis for applying empirical formulas and estimating water discharges in an ungauged channel. The values of discharges calculate for individual floods and cross-sections of riverbed can be used for 2D modelling. 2D modelling allows to estimate water velocity and shear stress. Dendrochronological indication with 2D modelling yields previously unavailable information on bank erosion in the past. Conducted research allowed not only to date past events of bank erosion and to estimate their magnitude, but also to estimate data on discharges, water velocity and shear stress during particular floods in an ungauged channel. Combined application of dendrochronology and hydraulic modelling based on empirical formulas allowed precise estimation of hydrodynamic parameters and erosion parameters. Results obtained from tree rings and 2D modelling can be used for preparing maps of flood hazard and risk.

CRediT authorship contribution statement

Ireneusz Malik: Conceptualization, Investigation. **Małgorzata Wistuba:** Writing - original draft. **Damian Absalon:** Supervision, Validation. **Michał Habel:** Methodology. **Sergey Chalov:** Data curation, Formal analysis. **Ruide Yu:** Investigation.

Declaration of Competing Interest

The authors declare that they have no known competing financial interests or personal relationships that could have appeared to influence the work reported in this paper.

Acknowledgements

References

Arbellay, E., Fonti, P., Stoffel, M., 2012. Duration and extension of anatomical changes in wood structure after cambial injury. J. Exp. Bot. 63 (8), 3271–3277. https://doi.org/10.1093/jxb/ers050.

Astrade, L., Bégin, Y., 1997. Tree-ring response of Populus tremula L. and Quercus robur L. to recent spring floods of the Saône River, France. Ecoscience 4 (2), 232–239. https://doi.org/10.1080/11956860.1997.11682400.

Baishya, S.J., 2013. A study on bank erosion by the River Baralia (Bhairatolajan) in Melkipara Village of Hajo Revenue Circle, Kamrup District, Assam, India. Int. J. Sci. Res. 3 (9), 1–10.

Ballesteros Cánovas, J.A., Eguibar, M., Bodoque, J.M., Díez-Herrero, A., Stoffel, M., Gutiérrez-Pérez, I., 2011. Estimating flash flood discharge in an ungauged mountain catchment with 2D hydraulic models and dendrogeomorphic palaeostage indicators. Hydrol. Process. 25 (6), 970–979. https://doi.org/10.1002/hyp.v25.610.1002/hyp.7888.

Ballesteros-Cánovas, J.A., Stoffel, M., St. George, S., Hirschboeck, K., 2015. A review of flood records from tree rings. Progr. Phys. Geogr.: Earth Environ. 39, 794–816. Geogr. doi: 10.1177/ 0309133315608758.

Bhuiyan, M.A.H., Kumamoto, T., Suzuki, S., 2015. Application of remote sensing and GIS for evaluation of the recent morphological characteristics of the lower Brahmaputra-Jamuna River, Bangladesh. Earth Sci. Inf. 8 (3), 551–568. https://doi.org/10.1007/s12145-014-0180-4.

Bodoque, J.M., Díez-Herrero, A., Martín-Duque, J.F., Rubiales, J.M., Godfrey, A., Pedraza, J., Carrasco, R.M., Sanz, M.A., 2005. Sheet erosion rates determined by using dendrogeomorphological analysis of exposed tree roots: Two examples from Central Spain. Catena 64 (1), 81–102. https://doi.org/10.1016/j.catena.2005.08.002.

Bollati, I., Della Seta, M., Pelfini, M., Del Monte, M., Fredi, P., Palmieri, E., 2012. Dendrochronological and geomorphological investigations to assess water erosion and mass wasting processes in the Apennines of Southern Tuscany (Italy). Catena 90, 1–17. https://doi.org/10.1016/j.catena.2011.11.005.

Bollschweiler, M., Stoffel, M., Schneuwly, D.M., 2008a. Dynamics in debris-flow activity on a forested cone – a case study using different dendroecological approaches. Catena 72 (1), 67–78. https://doi.org/10.1016/j.catena.2007.04.004.

Bollschweiler, M., Stoffel, M., Schneuwly, D.M., Bourqui, K., 2008b. Traumatic resin ducts in Larix decidua stems impacted by debris flows. Tree Physiol. 28 (2), 255–263. https://doi.org/10.1093/treephys/28.2.255.

Büchele, B., Kreibich, H., Kron, A., Thieken, A., Ihringer, J., Oberle, P., Merz, B., Nestmann, F., 2006. Flood-risk mapping: contributions towards an enhanced assessment of extreme events and associated risks. Nat. Hazard. Earth Syst. Sci. 6, 485–503. https://doi.org/10.5194/nhess-6-485-2006.

Büntgen, U., Frank, D., Liebhold, A., Johnson, D., Carrer, M., Urbinati, C., Grabner, M., Nicolussi, K., Levanic, T., Esper, J., 2009. Three centuries of insect outbreaks across

the European Alps. New Phytol. 182 (4), 929–941. https://doi.org/10.1111/nph.2009.182.issue-410.1111/j.1469-8137.2009.02825.x.

Carrara, P.E., Carroll, T.R., 1979. The determination of erosion rates from exposed tree roots in the Piceance Basin, Colorado. Earth Surf. Proc. Land. 4 (4), 307–317. https://doi.org/10.1002/(ISSN)1096-983710.1002/esp.v4:410.1002/esp.3290040402.

Casteller, A., Stoffel, M., Crespo, S., Villalba, R., Corona, C., Bianchi, E., 2015. Dendrogeomorphic reconstruction of flash floods in the Patagonian Andes. Geomorphology 228, 116–123. https://doi.org/10.1016/j.geomorph.2014.08.022.

Casteller, A., Stöckli, V., Villalba, R., Mayer, A.C., 2007. An evaluation of dendroecological indicators of snow avalanches in the Swiss Alps. Arctic Antarctic Alpine Res. 39, 218–228. doi: https://doi.org/10.1657/1523-0430(2007)39[218:AEODIO]2.0.CO;2.

Clark, L.A., Wynn, T.M., 2007. Methods for determining streambank critical shear stress and soil erodibility: implications for erosion rate predictions. Trans. – Am. Soc. Agric. Eng. 50, 95–106. https://doi.org/10.13031/2013.22415.

Corona, C., Lopez Saez, J., Rovéra, G., Stoffel, M., Astrade, L., Berger, F., 2011. High resolution, quantitative reconstruction of erosion rates based on anatomical changes in exposed roots at Draix, Alpes de Haute-Provence — critical review of existing approaches and independent quality control of results. Geomorphology 125 (3), 433–444. https://doi.org/10.1016/j.geomorph.2010.10.030.

Dean, J.S., 1988. Dendrochronology and paleoenvironmental reconstruction on the Colorado Plateaus. In: Gumerman, G.J. (Ed.), The Anasazi in a changing environment. Cambridge University Press, New York, pp. 119–167.

Derakhshannia, M., Dalvand, S., Asakereh, B., Askari, K.O.A., 2020. Corrosion and deposition in Karoon River Iran based on hydrometric stations. Int. J. Hydrol. Sci. Technol. 10 (4), 334. https://doi.org/10.1504/IJHST.2020.108264.

Di Baldassarre, G., Castellarin, A., Montanari, A., Brath, A., 2009. Probability-weighted hazard maps for comparing different flood risk management strategies: a case study. Nat. Hazard. 50 (3), 479–496. https://doi.org/10.1007/s11069-009-9355-6.

Elling, W., Dittmar, C., Pfaffelmoser, K., Rötzer, T., 2009. Dendroecological assessment of the complex causes of decline and recovery of the growth of silver fir (Abies alba Mill.) in Southern Germany. For. Ecol. Manage. 257 (4), 1175–1187. https://doi.org/10.1016/j.foreco.2008.10.014.

DHI, MIKE 21C, 2011. Curvilinear Model, Scientific Documentation, DHI Water & Environment.

Fantucci, R., 2007. Dendrogeomorphological analysis of shore erosion along Bolsena lake (Central Italy). Dendrochronologia 24 (2-3), 69–78. https://doi.org/10.1016/j.dendro.2006.11.002.

Gärtner, H., Schweingruber, F.H., Dikau, R., 2001. Determination of erosion rates by analyzing structural changes in the growth pattern of exposed roots. Dendrochronologia 19, 81–91.

Gärtner, H., 2007. Tree roots — methodological review and new development in dating and quantifying erosive processes. Geomorphology 86 (3-4), 243–251. https://doi.org/10.1016/j.geomorph.2006.09.001.

Gärtner, H., Nievergelt, D., 2010. The core-microtome: a new tool for surface preparation on cores and time series analysis of varying cell parameters. Dendrochronologia 28 (2), 85–92. https://doi.org/10.1016/j.dendro.2009.09.002.

Gärtner, H., Schweingruber, F.H., 2013. Microscopic preparation techniques for plant stem analysis. Verlag Dr, Kessel, Remagen.

Ghanem, A., Steffler, P., Hicks, F., Katopodis, C., 1996. Two-dimensional hydraulic simulation of physical habitat conditions in flowing streams. Regul. Rivers Res. Manage. 12, 185–200. https://doi.org/10.1002/(SICI)1099-1646(199603)12:2/33.0.CO;2-4.

Gholami, V., Chau, K., Fadaee, F., Torkaman, J., Ghaffari, A., 2015. Modeling of groundwater level fluctuations using dendrochronology in alluvial aquifers. J. Hydrol. 529, 1060–1069. https://doi.org/10.1016/j.jhydrol.2015.09.028.

Golian, M., Katibeh, H., Singh, V.P., Ostad-Ali-Askari, K., Rostami, H.T., 2020. Prediction of tunnelling impact on flow rates of adjacent extraction water wells. Q. J. Eng. Geol. Hydrogeol. 53 (2), 236–251. https://doi.org/10.1144/qjegh2019-055.

Grimaldi, S., Petroselli, A., Arcangeletti, E., Nardi, F., 2013. Flood mapping in ungauged basins using fully continuous hydrologic-hydraulic modelling. J. Hydrol. 487, 39–47. https://doi.org/10.1016/j.jhydrol.2013.02.023.

Hajdukiewicz, H., Wyżga, B., Mikuś, P., Zawiejska, J., Radecki-Pawlik, A., 2015. Impact of a large flood on mountain river habitats, channel morphology, and valley infrastructure. Geomorphology 272, 55–67. https://doi.org/10.1016/j.geomorph.2015.09.003.

Hankin, B., Metcalfe, P., Beven, K., Chappell, N., 2019. Integration of hillslope hydrology and 2D hydraulic modelling for natural flood management. Hydrol. Res. 50, 1535–1548. https://doi.org/10.2166/nh.2019.150.

Hassan, M.A., Church, M., Lisle, T.E., Brardinoni, F., Benda, L., Grant, G.E., 2005. Sediment transport and channel morphology of small, forested streams. J. Am. Water Resour. Assoc. 41 (4), 853–876. https://doi.org/10.1111/jawr.2005.41.issue-410.1111/j.1752-1688.2005.tb03774.x.

Harrison, S.S., Reid, J.R., 1967. A flood-frequency graph based on tree-scar data. Proceedings of the North Dakota. Acad. Sci. 21, 23–33.

Helley, E.J., LaMarche, V.C., 1968. December 1964, a 400-year flood in Northern California. U.S. Geol. Surv. Prof. Pap. 600D, 34–37.

Hitz, O.M., Gärtner, H., Heinrich, I., Monbaron, M., 2008. First time application of Ash (Fraxinus excelsior L.) roots to determine erosion rates in mountain torrents. Catena 72 (2), 248–258. https://doi.org/10.1016/j.catena.2007.05.008.

Horritt, M.S., Bates, P.D., 2002. Evaluation of 1D and 2D numerical models for predicting river flood inundation. J. Hydrol. 268 (1-4), 87–99. https://doi.org/10.1016/S0022-1694(02)00121-X.

Hunter, S.C., Allen, D.M., Kohfeld, K.E., 2020. Comparing approaches for reconstructing groundwater levels in the Mountainous Regions of Interior British Columbia,

Canada. Using Tree Ring Widths. Atmosphere 11, 1374. https://doi.org/10.3390/atmos11121374.

Jafarzadegan, K., Merwade, V.A., 2017. DEM-based approach for large-scale floodplain mapping in ungauged watersheds. J. Hydrol. 550, 650–662. https://doi.org/10.1016/j.jhydrol.2017.04.053.

Jämbäck, J., Heikkinen, O., Tuovinen, M., Autio, J., 1999. The effect of air-borne pollutants on the growth of Pinus sylvestris in the City of Oulu, Finland. Fennia 177, 161–169.

Kasprzak, M., 2010. Wezbrania i powodzie na rzekach Dolnego Śląska, in: Migoń P. (Ed.), Wyjątkowe zdarzenia przyrodnicze na Dolnym Śląsku i ich skutki. Rozprawy Naukowe Instytutu Geografii i Rozwoju Regionalnego Uniwersytetu Wrocławskiego, 14, 81–140. (in Polish: Floods on river of the Lower Silesia).

Kleinhans, M., 2005. Flow discharge and sediment transport models for estimating a minimum timescale of hydrological activity and channel and delta formation on Mars. J. Geophys. Res. 110, E12003. https://doi.org/10.1029/2005JE002521.

Konter, O., Esper, J., Liebhold, A., Kyncl, T., Schneider, L., Düthorn, E., Büntgen, U., 2015. Tree-ring evidence for the historical absence of cyclic larch budmoth outbreaks in the Tatra Mountains. Trees-Structure and Function 29 (3), 809–814. https://doi.org/10.1007/s00468-015-1160-0.

LaMarche, V.C., 1966. An 800-year history of stream erosion as indicated by botanical evidence. U.S. Geol. Surv. Prof. Pap. 550D, 83–86.

Llasat, M.D.C., Rigo, T., Barriendos, M., 2003. The 'Montserrat-2000' flash-flood event: A comparison with the floods that have occurred in the northeastern Iberian Peninsula since the 14th century. Int. J. Climatol. 23 (4), 453–469. https://doi.org/10.1002/(ISSN)1097-008810.1002/joc.v23:410.1002/joc.888.

Lane, S.N., Ferguson, R.I., 2005. Modelling reach-scale fluvial flows. In: Bates, P.D., Lane, S.N., Ferguson, R.I. (Eds.), Computational Fluid Dynamics: Applications in Environmental Hydraulics. John Wiley & Sons Ltd., pp. 217–269. https://doi.org/10.1002/0470015195.ch10.

Lawler, D.M., 1993. The measurement of river bank erosion and lateral channel change: a review. Earth Surf. Proc. Land. 18 (9), 777–821. https://doi.org/10.1002/(ISSN)1096-983710.1002/esp.v18:910.1002/esp.3290180905.

Malik, I., 2006. Contribution to understanding the historical evolution of meandering rivers using dendrochronological methods: Example of the Mała Panew River in southern Poland. Earth Surf. Process. Landform 31 (10), 1227–1245. https://doi.org/10.1002/(ISSN)1096-983710.1002/esp.v31:1010.1002/esp.1331.

Malik, I., 2008. Dating of small gully formation and establishing erosion rates in old gullies under forest by means of anatomical changes in exposed tree roots (southern Poland). Geomorphology 93, 421–436. https://doi.org/10.1016/j.geomorph.2007.03.007.

Malik, I., Matyja, M., 2008. Bank erosion history of a mountain stream determined by means of anatomical changes in exposed tree roots over the last 100years (Bila Opava River — Czech Republic). Geomorphology 98, 126–142. https://doi.org/10.1016/j.geomorph.2007.02.030.

Malik, I., Danek, M., Marchwińska-Wyrwał, E., Danek, T., Wistuba, M., Krąpiec, M., 2012. Scots pine (Pinus sylvestris L.) growth suppression and adverse effects on human health due to air pollution in the Upper Silesian Industrial District (USID), southern Poland. Water, Air, Soil Pollution 223 (6), 3345–3364. https://doi.org/10.1007/s11270-012-1114-8.

Malik, I., Wistuba, M., 2012. Dendrochronological methods for reconstructing mass movements — an example of landslide activity analysis using tree-ring eccentricity. Geochronometria 39, 180–196. https://doi.org/10.2478/s13386-012-0005-5.

Malik, I., Pawlik, Ł., Ślęzak, A., Wistuba, M., 2019. A study of the wood anatomy of Picea abies roots and their role in biomechanical weathering of rock cracks. Catena 173, 264–275. https://doi.org/10.1016/j.catena.2018.10.018.

Manning, R., 1891. On the flow of water in open channels and pipes. Trans. Inst. Civil Eng. Ireland 20, 161–207.

Marchi, L., Borga, M., Preciso, E., Gaume, E., 2010. Characterisation of selected extreme flash floods in Europe and implications for flood risk management. J. Hydrol. 394 (1-2), 118–133. https://doi.org/10.1016/j.jhydrol.2010.07.017.

Masood, M., Takeuchi, K., 2012. Assessment of flood hazard, vulnerability and risk of mideastern Dhaka using DEM and 1D hydrodynamic model. Nat. Hazard. 61 (2), 757–770. https://doi.org/10.1007/s11069-011-0060-x.

Matakiewicz, M., 1905. Versuch der Aufstellung einer Geschwindigkeitsformel für natürliche Flußbette. Sonderabdruck aus der "Österreichischen Wochenschrift für den öffentlichen Baudienst", Heft 51.

Mazzorana, B., Comiti, F., Fuchs, S., 2013. A structured approach to enhance flood hazard assessment in mountain streams. Nat. Hazard. 67 (3), 991–1009. https://doi.org/10.1007/s11069-011-9811-y.

Merz, B., Kreibich, H., Schwarze, R., Thieken, A., 2010. Review article 'Assessment of economic flood damage'. Nat. Hazard. Earth Syst. Sci. 10, 1697–1724. https://doi.org/10.5194/nhess-10-1697-2010.

Migoń, P., Hrádek, M., Parzóch, K., 2002. Extreme events in the Sudetes Mountains. Their long-term geomorphic impact and possible controlling factors. Studia Geomorphologica Carpatho-Balcanica 36, 29–49.

Mili, N., Acharjee, S., Konwar, M., 2013. Impact of flood and river bank erosion on socio economy: a case study of Golaghat revenue circle of Golaghat district, Assam. Int. J. Geol. Earth Environ. Sci. 3, 180–185. doi: http://www.cibtech.org/jgee.htm.

de Moel, H., van Alphen, J., Aerts, J.C.J.H., 2009. Flood maps in Europe - methods, availability and use. Nat. Hazard. Earth Syst. Sci. 9 (289–301), 2009. https://doi.org/10.5194/nhess-9-289-2009.

Morianou, G.G., Kourgialas, N.N., Karatzas, G.P., 2016. Comparison between curvilinear and rectilinear grid based hydraulic models for river flow simulation. Procedia Eng. 162, 568–575. https://doi.org/10.1016/j.proeng.2016.11.102.

Morianou, G.G., Kourgialas, N.N., Karatzas, G.P., Nikolaidis, N.P., 2018. Assessing hydro-morphological changes in Mediterranean stream using curvilinear grid modeling

approach - climate change impacts. Earth Sci. Inf. 11 (2), 205–216. https://doi.org/10.1007/s12145-017-0326-2.

Neuvel, J.M.M., van den Brink, A., 2009. Flood risk management in Dutch local spatial planning practices. J. Environ. Plann. Manage. 52 (7), 865–880. https://doi.org/10.1080/09640560903180909.

Norbiato, D., Borga, M., Degli Esposti, S., Gaume, E., Anquetin, S., 2008. Flash flood warning based on rainfall depth-duration thresholds and soil moisture conditions: an assessment for gauged and ungauged basins. J. Hydrol. 362, 274–290. https://doi.org/10.1016/j.jhydrol.2008.08.023.

O'Brien, JD., 2006. FLO-2D User's Manual, Version 2006.01. FLO Engineering, Nutrioso.

Ostad-Ali-Askari, K., Shayannejad, M., 2021. Quantity and quality modelling of groundwater to manage water resources in Isfahan-Borkhar Aquifer. Environ. Dev. Sustain. 1–17 https://doi.org/10.1007/s10668-021-01323-1.

Ostad-Ali-Askari, K., Ghorbanizadeh Kharazi, H., Shayannejad, M., Zareian, M.J., 2019. Effect of management strategies on reducing negative impacts of climate change on water resources of the Isfahan-Borkhar aquifer using MODFLOW. River Res. Appl. 35 (6), 611–631. https://doi.org/10.1002/rra.v35.610.1002/rra.3463.

Ostad-Ali-Askari, K, Ghorbanizadeh-Kharazi, H., Shayannejad, M, Zareian, M.J., 2020. Effect of climate change on precipitation patterns in an arid region using GCM models: case study of Isfahan-Borkhar plain. Nat. Hazard. Rev. 21, 04020006. doi: https://doi.org/10.1061/(ASCE)NH.1527-6996.0000367.

Ostad-Ali-Askari, K., Shayannejad, M., Ghorbanizadeh-Kharazi, H., 2017. Artificial neural network for modeling nitrate pollution of groundwater in marginal area of Zayandeh-rood River, Isfahan, Iran. KSCE J. Civil Eng. 21 (1), 134–140. https://doi.org/10.1007/s12205-016-0572-8.

Parzóch, K., Dunajski, A., 2002. Katastrofalne ruchy masowe w Karkonoskim Parku Narodowym związane z nadmiernymi opadami, in: Denisiuk, Z., (Ed.), Strategia zachowania różnorodności biologicznej i krajobrazowej obszarów przyrodniczo cennych dotkniętych klęską powodzi, Instytut Ochrony Przyrody PAN, 155-165, (in Polish: Catastrophic mass movements in the Karkonosze National Park related to heavy precipitation).

Pasternack, G.B., Gilbert, A.T., Wheaton, J.M., Buckland, E.M., 2006. Error propagation for velocity and shear stress prediction using 2D models for environmental management. J. Hydrol. 328 (1-2), 227–241. https://doi.org/10.1016/j.jhydrol.2005.12.003.

Pasternack, G.B., Senter, A.E., 2011. 21st century instream flow assessment framework for mountain streams (CEC–500–2013–059). California Energy Commission, PIER, Sacramento, CA.

Pasternack, G.B., Wyrick, J.R., 2016. Flood–driven topographic changes in a gravel–cobble river over segment, reach, and unit scales. Earth Surf. Proc. Land. 42, 487–502. https://doi.org/10.1002/esp.4064.

Pelfini, M., Santilli, M., 2006. Dendrogeomorphological analyses on exposed roots along two mountain hiking trails in the Central Italian Alps. Geogr. Ann. 88 (3), 223–236. https://doi.org/10.1111/j.1468-0459.2006.00297.x.

Pirnazar, M., Hasheminasab, H., Karimi, A.Z., Ostad-Ali-Askari, K., Ghasemi, Z., Hamedani, M.H., Esfahani, E.M., Eslamian, S., 2018. The evaluation of the usage of the fuzzy algorithms in increasing the accuracy of the extracted land use maps. Int. J. Glob. Environ. Issues 17, 307–321. https://doi.org/10.1504/IJGENVI.2018.095063.

Reid, H.E., Williams, R.D., Brierley, G.J., Coleman, S.E., Lamb, R., Rennie, C.D., Tancock, M.J., 2019. Geomorphological effectiveness of floods to reworkgravel bars: insight from hyperscale topography and hydraulic modelling. Earth Surf. Proc. Land. 44 (2), 595–613. https://doi.org/10.1002/esp.v44.210.1002/esp.4521.

Rosgen, D.L., 1994. A classification of natural rivers. Catena 22 (3), 169–199. https://doi.org/10.1016/0341-8162(94)90001-9.

Ruiz-Villanueva, V., Díez-Herrero, A., Stoffel, M., Bollschweiler, M., Bodoque, J.M., Ballesteros, J.A., 2010. Dendrogeomorphic analysis of flash floods in a small ungauged mountain catchment (Central Spain). Geomorphology 118 (3-4), 383–392. https://doi.org/10.1016/j.geomorph.2010.02.006.

Salehi-Hafshejani, S., Shayannejad, M., Samadi-Broujeni, H., Zarraty, A.R., Soltani, B., Mohri-Esfahani, E., Haeiri-Hamedani, M., Eslamian, S., Ostad-Ali-Askari, K., 2019. Determination of the height of the vertical filter for heterogeneous Earth dams with vertical clay core. Int. J. Hydrol. Sci. Technol. 9, 221. https://doi.org/10.1504/IJHST.2019.102315.

Schweingruber, F.H., 1996. Tree rings and Environment. Dendroecology. Swiss Federal Institute for Forests, Snow and Landscape Research, WSL/FNP Birmensdorf. Paul Haupt Publishers Berne, Stuttgart, Vienna.

Šilhán, K., 2015. Frequency, predisposition, and triggers of floods in flysch Carpathians: Regional study using dendrogeomorphic methods. Geomorphology 234, 243–253. https://doi.org/10.1016/j.geomorph.2014.12.041.

Sigafoos, R.S., 1964. Botanical evidence of floods and flood-plain deposition. U.S. Geol. Surv. Prof. Pap. 485A, 1–35.

Shen, Y.i., Diplas, P., 2008. Application of two-and three-dimensional computational fluid dynamics models to complex ecological stream flows. J. Hydrol. 348 (1-2), 195–214. https://doi.org/10.1016/j.jhydrol.2007.09.060.

Smagorinsky, J., 1963. General circulation experiments with the primitive equations. Mon. Weather Rev. 91, 99–164. https://doi.org/10.1175/1520-0493(1963)091<0099:GCEWTP>2.3.CO;2.

Stoffel, M., Casteller, A., Luckman, B.H., Villalba, R., 2012. Spatiotemporal analysis of channel wall erosion in ephemeral torrents using tree roots — an example from the Patagonian Andes. Geology 40, 247–250. https://doi.org/10.1130/G32751.1.

Stoffel, M., Corona, C., Ballesteros-Cánovas, J.A., Bodoque, J.M., 2013. Dating and quantification of erosion processes based on exposed roots. Earth Sci. Rev. 123, 18–34. https://doi.org/10.1016/j.earscirev.2013.04.002.

Tarekegn, T.H., Haile, A., Rientjes, T., Reggiani, P., Alkema, D., 2010. Assessment of an ASTER-generated DEM for 2D hydrodynamic flood modelling. Int. J. Appl. Earth Obs. Geoinf. 12, 457–465. https://doi.org/10.1016/j.jag.2010.05.007.

Tongbi, T., Carr, K., Ercan, A., Trinh, T., Nosacka, J., 2017. Assessment of the effects of multiple extreme floods on flow and transport processes under competing flood protection and environmental management strategies. Sci. Total Environ. 607–608, 613–622. doi: 10.1016/j.scitotenv.2017.06.271.

Vandekerckhove, L., Poesen, J., Oostwoud Wijdenes, D., Gyssels, G., 2001a. Short-term bank gully retreat rates in Mediterranean environments. Catena 44 (2), 133–161. https://doi.org/10.1016/S0341-8162(00)00152-1.

Vandekerckhove, L., Muys, B., Poesen, J., De Weerdt, B., Coppe, N., 2001b. A method for dendrochronological assessment of medium-term gully erosion rates. Catena 45, 123–161. https://doi.org/10.1016/S0341-8162(00)00152-1.

Vinet, F., 2008. Geographical analysis of damage due to flash floods in southern France: the cases of 12–13 November 1999 and 8–9 September 2002. Appl. Geogr. 28 (4), 323–336. https://doi.org/10.1016/j.apgeog.2008.02.007.

Wertz, E.L., St. George, S., Zeleznik, J.D., 2013. Vessel anomalies in Quercus macrocarpa tree rings associated with recent floods along the Red River of the North, United States. Water Resour. Res. 49 (1), 630–634. https://doi.org/10.1029/2012WR012900.

Wistuba, M., Malik, I., Gärtner, H., Kojs, P., Owczarek, P., 2013. Application of eccentric growth of trees as a tool for landslide analyses: The example of Picea abies Karst. In the Carpathian and Sudeten Mountains (Central Europe). Catena 111, 41–55. https://doi.org/10.1016/j.catena.2013.06.027.

Wu, Y., Cheng, H., 2005. Monitoring of gully erosion on the Loess Plateau of China using a global positioning system. Catena 63 (2-3), 154–166. https://doi.org/10.1016/j.catena.2005.06.002.

Wu, W., Jiang, E., China, P.R., Wang, S.S.Y., 2004. Depth averaged 2D calculation of flow and sediment transport in the lower Yellow River. J. Hydraul. Res. 2 (1), 51–59. https://doi.org/10.1080/15715124.2004.9635221.

Wu, W., Shields, F.D., Bennett, S.J., Wang, S.S., 2005. A depth-averaged two-dimensional model for flow, sediment transport, and bed topography in curved channels with riparian vegetation. Water Resour. Res. 41, W03015. https://doi.org/10.1029/2004WR003730.

Yanosky, T.M., 1984. Documentation of high summer flows on the Potomac River from the wood anatomy of ash trees. Water Resour. Bull. 20, 241–250. https://doi.org/10.1111/j.1752-1688.1984.tb04678.xd.

Yumoto, M., Ishida, S., Fukazawa, K., 1983. Studies on the formation and structure of the compression wood cells induced by artifactual initiation in young trees of Picea glauca. IV. Gradation of the severity of compression wood tracheids. Res. Bull. College Experiment For. 40, 409–454.

Zielonka, T., Holeksa, J., Ciapała, S., 2008. A reconstruction of flood events using scarred trees in the Tatra Mountains, Poland. Dendrochronologia 26 (3), 173–183. https://doi.org/10.1016/j.dendro.2008.06.003.

Zhou, H., Chen, Y., Hao, X., Zhao, Y., Fang, G., Yang, Y., 2019. Tree rings: a key ecological indicator for reconstruction of groundwater depth in the lower Tarim River, Northwest China. Ecohydrology 12 (8). https://doi.org/10.1002/eco.v12.810.1002/eco.2142.